

## MULTICOLOR *UBVRI* POLARIMETRY OF NGC 4755 AND THE $\beta$ CEPHEI POPULATION<sup>1</sup>

E. Irene Vega,<sup>2,4</sup> Ana María Orsatti,<sup>3,4</sup> and Ruben E. Martínez<sup>2,3</sup>

Received April 1 2014; accepted September 2 2014

### RESUMEN

Se presentan observaciones polarimétricas en las bandas *UBVRI* de 66 estrellas situadas en la dirección del cúmulo NGC 4755, incluyendo once  $\beta$  Cephei. Casi la mitad de estas variables muestran indicios de polarización intrínseca, pero según la teoría ninguna clase de pulsación puede originarla. Del análisis de las principales características de sus curvas  $P_V$  vs.  $\lambda_V$  hemos encontrado posibles orígenes de la dispersión de la luz en atmósferas extendidas, así como sospechas de binaridad en algunos casos. La polarización media para los miembros de NGC 4755 es  $P_V = 2.76\%$ , con  $\theta_V = 76^\circ.6$ . Las partículas tienen un tamaño medio normal para el ISM, y la eficiencia es elevada. Con el uso exclusivo de herramientas polarimétricas se han identificado un total de 25 estrellas miembro.

### ABSTRACT

We present *UBVRI* polarimetric observations of 66 stars in the direction of NGC 4755, including eleven  $\beta$  cephei stars. About half of these variables show indications of intrinsic polarization, but according to the theory neither radial nor non-radial pulsations could cause such polarizations. From the main characteristics of their  $P_V$  vs.  $\lambda_V$  curves we found as a possible origin, in some cases, scattering of light in extended atmospheres and suspected binarity, in some cases. The parameters of the interstellar medium towards the cluster are  $P_V = 2.76 \pm 0.13(\%)$  and  $\theta_V = 76^\circ.6 \pm 0^\circ.9$ ; the mean wavelength of maximum polarization amounts to  $0.56 \pm 0.04 \mu\text{m}$ . The value of polarization efficiency is higher than the mean, indicating a good alignment of the dust particles. A total of 25 stars were identified as members of NGC 4755; the identification task was improved through the use of polarimetric tools.

*Key Words:* ISM: dust, extinction — open clusters and associations: NGC 4755; stars: variables:  $\beta$  Cephei

### 1. INTRODUCTION

Since 1994, the polarimetric team at the La Plata Observatory has carried out systematic observations of a large number of Galactic open clusters, identifying twenty objects up to now. The polarimetric

technique is a very useful tool to obtain significant information about dust located in front of a luminous object: magnetic field direction,  $\lambda_{max}$ ,  $P_{\lambda_{max}}$ , and other parameters. Open clusters are very good candidates for polarimetric observations, because many of them have been studied through photometric and spectroscopic techniques and detailed information on the color, luminosity, spectral type and other properties of their stars is readily available. By combining this information, not only can the physical parameters of the cluster and its members be obtained, but also the distribution, size and efficiency of the dust grains that polarize the starlight. Besides, it is also possible to detect the presence (if any) of intraclus-

<sup>1</sup>Based on observations obtained at Complejo Astronómico El Leoncito, operated under agreement between the Consejo Nacional de Investigaciones Científicas y Técnicas de la República Argentina and the Universities of La Plata, Córdoba, and San Juan.

<sup>2</sup>Facultad de Ciencias Astronómicas y Geofísicas, Observatorio Astronómico, La Plata, Argentina.

<sup>3</sup>Instituto de Astrofísica de La Plata (UNLP- CONICET), Fac. de Cs. Astronómicas y Geofísicas, Argentina.

<sup>4</sup>Member of the Carrera del Investigador Científico, CONICET, Argentina.

ter dust, and with additional observations of non-member stars in the same region, to investigate the interstellar dust distribution in the direction of the cluster and the different directions of the Galactic magnetic field along the line of sight to the object.

In this work, we selected the southern open cluster NGC 4755 ( $l=303^\circ 2$ ,  $b=+2^\circ 5$ ), also known as Herschel’s “Jewel Box”, a young open cluster with an angular diameter of about  $10'$ , where the most brilliant stars concentrate (Lynga 1987). Many photometric and spectroscopic studies have been focused on the cluster, e.g.: (Arp & van Sant 1958), (Hernández 1960), (Feast 1963), (Schild 1970), (Dachs & Kaiser 1984), (Sagar & Cannon 1995), (Evans et al. 2005), (Bonatto et al. 2006), (Aidelman et al. 2012), and others. The distances found for this cluster range from 0.83 kpc (Arp & van Sant 1958) to 2.63 kpc (Aidelman et al. 2012); these discrepancies could be strongly related to the reddening measurements, as suggested by (Aidelman et al. 2012). In addition, according to the evolutionary model used by those authors, ages in the range 3 to 11.2 Myr were found. The deep *UBVRI* CCD photometry of (Sagar & Cannon 1995) resulted in an excess  $E_{B-V} = 0.41$  and a small differential reddening range of 0.05 throughout the field of NGC 4755. This is in accordance with (Bonatto et al. 2006), who found no evidence of gas emission or dust filaments, which they attribute to a post-embedded young open cluster where molecular and dust clouds are dissipating.

Many different types of variables are present in the cluster, among them  $\beta$  Cephei stars. In their catalog, (Stankov & Handler 2005) define these variables as massive stars with spectral type O or B whose light, radial velocity and/or line profile variations are caused by low-order pressure and gravity mode pulsations. Many are part of known multiple systems with physically associated companions and have preference for open clusters; NGC 3293 and NGC 4755 have the highest numbers.  $\beta$  Cephei may present radial and non-radial oscillations. If the pulsation mode is radial, then the polarization is predicted to remain constant over the photometric period (Serkowski 1968, 1970). But the distortion of the surface undergoing non-radial pulsations should produce a varying net polarization due to electron scattering (Odell 1979, Watson 1983). According to Clarke (1986), the pulsator may exhibit a sinusoidal polarization behavior as a function of the pulsational phase, with very low amplitude. Our observations were not spread over time nor have we looked for

TABLE 1  
*UBV(RI)<sub>KC</sub>*

Filter	$\lambda_{eff}(\mu\text{m})$
<i>U</i>	0.36
<i>B</i>	0.43
<i>V</i>	0.55
<i>R</i> (KC)	0.63
<i>I</i> (KC)	0.78

KC: Kron-Cousins

variability. Instead, we used possible departures of the polarization data from Serkowski’s law as evidence of intrinsic polarization.

## 2. OBSERVATIONS

Observations in the *UBV(RI)<sub>KC</sub>* bands (KC:Kron-Cousins), whose  $\lambda_{eff}$  in microns are listed in Table 1, were carried out using the rotating plate polarimeter CASPROF attached to the 2.15 m telescope at the Complejo Astronómico El Leoncito (San Juan, Argentina). This instrument is an improvement of the original design of the photoelectric polarimeter known as VATPOL (Magalhães et al. 1984) and takes advantage of two high throughput photocells (Martínez et al. 1990). CASPROF provides 6 diaphragms for polarimetric use, which in combination with the 2.15 m telescope, result in apertures of 5.0, 11.3, 17.0, 22.6, 33.9, and 45.2 arcsecs. Standard stars from (Turnshek et al. 1990) and from (Hsu & Breger 1982) were observed several times in every run to try to determine both the instrumental polarization (less than 0.02% in the entire set of filters) and the zero point of the polarization angle system.

## 3. RESULTS

The observation of 66 stars in the direction of NGC 4755 was performed in the years 1998 to 2003, in common with other projects. They are listed in Table 2 which shows, in self-explanatory format, the stellar identification, the polarization percentage ( $P_\lambda$ ), the position angle of the electric vector ( $\theta_\lambda$ ) in the equatorial coordinate system, and the respective mean errors for each filter computed considering the photon shot noise as the dominant source of errors (Maronna et al. 1992). Stellar identifications were taken from (Arp & van Sant 1958; capital letters),

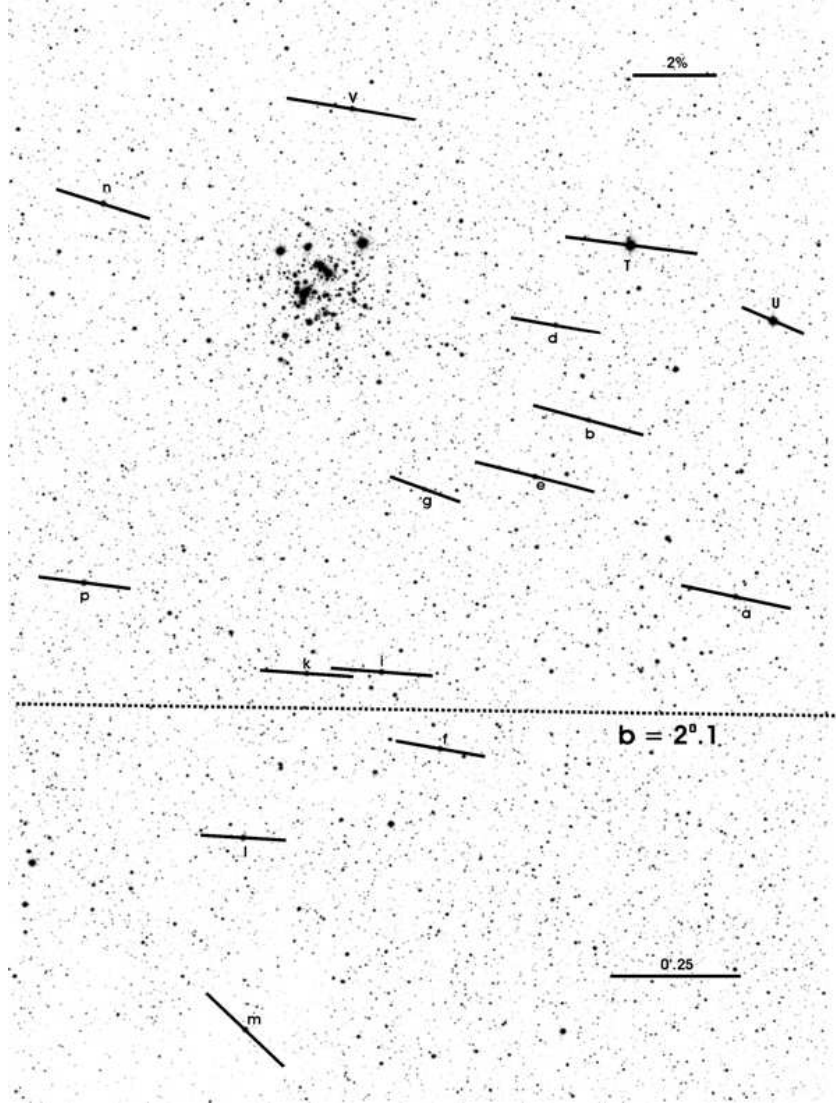


Fig. 1. Projection on the sky of the polarization vectors (Johnson V-filter) of the stars observed in the region of NGC 4755, where the dot-dashed line is the Galactic parallel  $b = +2^{\circ}.10$ ; the length of each vector is proportional to the polarization percentage and the image is from NASA's SkyView.

and from (Dachs & Kaiser 1984; small letters); for the rest we used the star numbers given by the above-mentioned authors, converted into three-figure numbers following (Dachs & Kaiser 1984). Additional identifications are also provided.

The sky projection of the V-band polarization vectors for the stars observed in NGC 4755 is shown in Figure 1 for the cluster region and in Figure 2 for the cluster itself. The dashed lines superimposed to both figures indicate the orientation of the projection of the Galactic plane onto the region. Most of the polarization vectors are not completely aligned with this direction: the usual finding when we deal with

a relatively young open cluster, where dust particles did not have enough time to relax and polarize the light in the same orientation as the GP in the region (Axon & Ellis 1976).

## 4. ANALYSIS AND DISCUSSION

### 4.1. *Fitting Serkowski's law*

Elongated dust grains in the interstellar medium, aligned because of the Galactic magnetic field, can produce a preferred orientation of the polarization. Serkowski noted that observations of interstellar polarization for all the stars follow the same curve, well

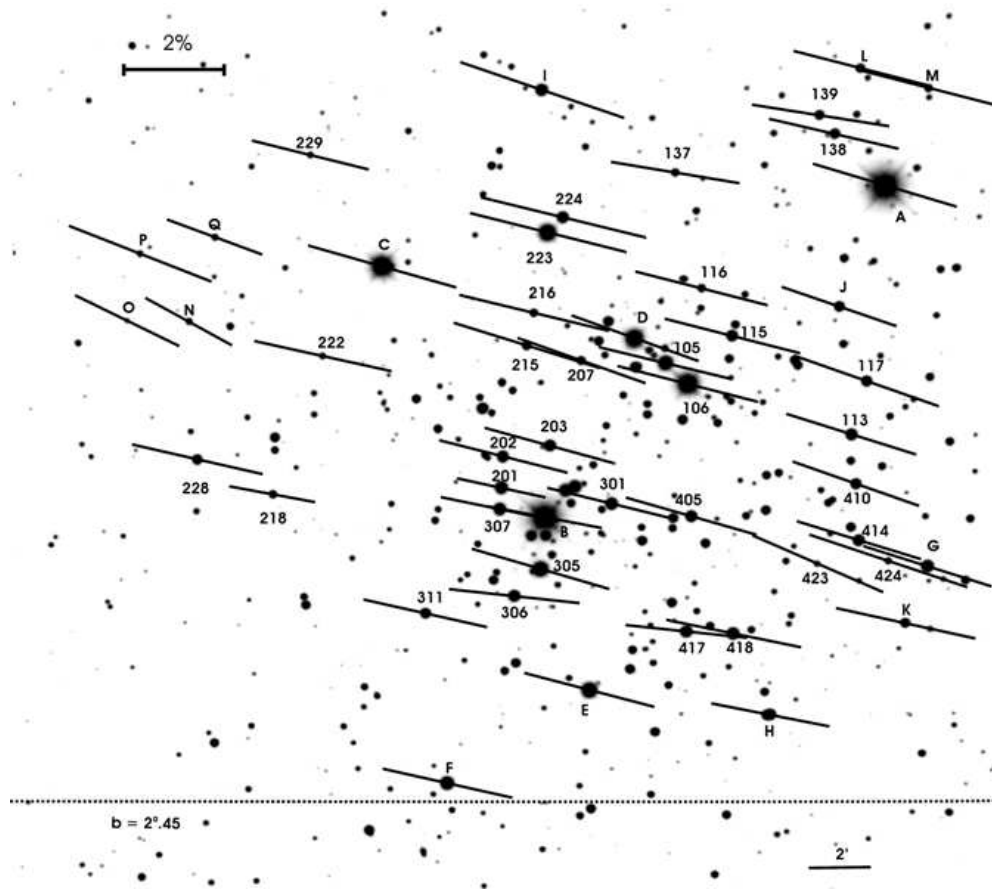


Fig. 2. The projected polarization vectors for the cluster, where the line indicates the Galactic parallel  $b = +2^\circ.45$ . The length of each vector is proportional to the polarization percentage and the image is from [http://www.noao.edu/image\\\_gallery/html/im0423.html](http://www.noao.edu/image\_gallery/html/im0423.html).

approximated by an empirical formula (Serkowski 1973). To analyze the data, the observations in the five filters were fitted for each star of our sample using Serkowski's law of interstellar polarization given by

$$P_\lambda/P_{\lambda_{max}} = e^{-Kln^2(\lambda_{max}/\lambda)} \quad (1)$$

If polarization is produced by aligned interstellar dust particles, we assume that the observed data (in terms of wavelength within the *UBVRI* bands) will then follow equation (1) and each star will have a  $P_{\lambda_{max}}$  and a  $\lambda_{max}$  value. To perform the fitting, we adopted  $K = 1.66\lambda_{max} + 0.01$  (Whittet et al. 1992), where  $\lambda_{max}$  is in  $\mu\text{m}$ . The individual  $P_{\lambda_{max}}$ ,  $\lambda_{max}$  values, spectral types from the literature, and the star identification, are listed in Table 3.

Intrinsic stellar polarizations may be distinguished from the interstellar component by time variability, by a wavelength dependence different from that of interstellar polarization, and/or by a

strong rotation of polarization position angle with wavelength. Two important polarizing mechanisms may cause linear intrinsic polarization: scattering in a flattened plasma disk around Ae/Be stars (Serkowski 1968, Coyne & Kruszewski 1969, etc.), and light scattering by large size grains located in non-spherically distributed dust clouds, as in the light from red giants, red and yellow variables, and other objects (Coyne & Vrba 1976, Bergeat et al. 1976, etc.). There are also combinations of both mechanisms acting on the light of single stars (e.g. Capps, Coyne & Dick 1973; HD 44179) and binary stars, especially close binaries: these contain mass transfer streams, hot spots where the stream falls into the accretion disk around the gainer star, and an asymmetric donor star. Each of these components represents an asymmetry that contributes to the net polarization (Bjorkman 2011).

To detect if a particular star displays indications of non-interstellar polarization, we computed the  $\sigma_1$

TABLE 2  
POLARIMETRIC OBSERVATIONS IN THE OPEN CLUSTER NGC 4755

Star <sup>a</sup>	HD/CPD <sup>b</sup>	GCVS/ <sup>c</sup> NSVS	Filter	$P_{\lambda} \pm \epsilon_P$ %	$\theta_{\lambda} \pm \epsilon_{\theta}$ °	Star <sup>a</sup>	HD/CPD <sup>b</sup>	GCVS/ <sup>c</sup> NSVS	Filter	$P_{\lambda} \pm \epsilon_P$ %	$\theta_{\lambda} \pm \epsilon_{\theta}$ °
A	111904	6008	<i>U</i>	2.47±0.06	76.1±0.7	I	-59°4550	CV Cru	<i>U</i>	2.65±0.06	73.0±0.7
			<i>B</i>	2.85±0.03	74.0±0.3				<i>B</i>	3.06±0.09	72.2±0.9
			<i>V</i>	3.04±0.02	73.7±0.2				<i>V</i>	3.20±0.07	73.4±0.6
			<i>R</i>	2.88±0.02	73.8±0.2				<i>R</i>	3.30±0.09	71.7±0.8
			<i>I</i>	2.54±0.02	74.2±0.3				<i>I</i>	3.09±0.09	71.1±0.8
B	111973	19540	<i>U</i>	2.07±0.08	75.4±1.1	J	-59°4537	<i>U</i>	1.96±0.08	73.3±1.2	
			<i>B</i>	2.37±0.09	76.1±1.1			<i>B</i>	2.35±0.06	68.1±0.8	
			<i>V</i>	2.34±0.06	79.2±0.7			<i>V</i>	2.46±0.05	71.1±0.6	
			<i>R</i>	2.42±0.06	76.9±0.7			<i>R</i>	2.48±0.04	69.5±0.5	
			<i>I</i>	2.35±0.12	76.9±1.4			<i>I</i>	1.98±0.10	70.1±1.5	
C	111990	19543	<i>U</i>	2.52±0.15	73.4±1.7	K	-59°4530	<i>U</i>	2.48±0.16	73.4±1.8	
			<i>B</i>	2.87±0.12	73.6±1.2			<i>B</i>	2.97±0.09	74.6±0.9	
			<i>V</i>	3.12±0.14	74.2±1.3			<i>V</i>	2.89±0.09	77.7±0.9	
			<i>R</i>	3.04±0.12	73.1±1.1			<i>R</i>	2.64±0.07	74.7±0.8	
			<i>I</i>	3.16±0.18	68.4±1.6			<i>I</i>	2.28±0.07	74.7±0.9	
D	-59°4547	DU Cru	<i>U</i>	3.05±0.60	74.7±5.6	L	19528	<i>U</i>	...	...	
			<i>B</i>	2.67±0.13	73.2±1.4			<i>B</i>	2.50±0.06	77.8±0.7	
			<i>V</i>	2.73±0.03	70.2±0.3			<i>V</i>	2.81±0.11	75.6±1.2	
			<i>R</i>	2.71±0.02	72.9±0.2			<i>R</i>	2.92±0.10	76.9±1.0	
			<i>I</i>	2.45±0.02	74.6±0.2			<i>I</i>	2.47±0.11	72.5±1.3	
E	-59°4552		<i>U</i>	2.37±0.05	77.8±0.6	M	19521	<i>U</i>	3.01±0.56	67.2±5.3	
			<i>B</i>	2.56±0.03	76.4±0.3			<i>B</i>	3.42±0.16	80.3±1.3	
			<i>V</i>	2.72±0.03	75.4±0.3			<i>V</i>	3.02±0.14	69.4±1.3	
			<i>R</i>	2.67±0.02	75.7±0.2			<i>R</i>	2.77±0.14	78.3±1.5	
			<i>I</i>	2.47±0.02	76.0±0.2			<i>I</i>	2.65±0.11	73.9±1.2	
F	-59°4564	BW Cru	<i>U</i>	2.81±0.24	52.6±2.5	N	<i>U</i>	1.92±0.36	71.0±5.4		
			<i>B</i>	2.37±0.11	75.4±1.3		<i>B</i>	2.07 ±0.29	67.7±1.7		
			<i>V</i>	2.69±0.10	77.4±1.0		<i>V</i>	2.00 ±0.19	61.3±1.2		
			<i>R</i>	2.59±0.07	75.7±0.8		<i>R</i>	1.84 ±0.21	65.5±1.1		
			<i>I</i>	2.25±0.17	75.0±2.1		<i>I</i>	1.31 ±0.21	59.5±2.8		
G	-59°4528	BS Cru	<i>U</i>	2.23±0.05	71.7±0.7	O	<i>U</i>	1.67±0.32	73.9±5.4		
			<i>B</i>	2.71±0.06	73.3±0.6		<i>B</i>	2.58±0.11	70.9±1.2		
			<i>V</i>	2.72±0.04	72.8±0.4		<i>V</i>	2.34±0.13	64.0±1.6		
			<i>R</i>	2.72±0.04	70.8±0.4		<i>R</i>	2.45±0.12	71.1±1.3		
			<i>I</i>	2.34±0.08	71.2±1.0		<i>I</i>	2.31±0.11	70.3±1.4		
H	-59°4540	19537	<i>U</i>	2.05±0.13	77.2±1.8	P	<i>U</i>	2.68±0.27	71.6±2.8		
			<i>B</i>	1.98±0.17	77.1±2.4		<i>B</i>	2.64±0.10	74.8±1.1		
			<i>V</i>	2.44±0.11	79.0±1.3		<i>V</i>	3.10±0.12	68.9±1.1		
			<i>R</i>	2.35±0.16	75.6±1.9		<i>R</i>	2.74±0.11	67.8±1.2		
			<i>I</i>	2.32±0.22	80.6±2.6		<i>I</i>	2.65±0.13	67.7±1.4		
Q			<i>U</i>	2.94 ±0.34	61.3±5.4	f	111825	<i>U</i>	1.86±0.10	87.5±1.5	
			<i>B</i>	2.28 ±0.22	73.6±1.5			<i>B</i>	2.00±0.12	78.6±1.7	
			<i>V</i>	2.05 ±0.18	69.8±0.9			<i>V</i>	2.15±0.08	79.5±1.1	
			<i>R</i>	2.03 ±0.19	70.8±1.2			<i>R</i>	2.07±0.16	80.3±2.2	
			<i>I</i>	1.77 ±0.29	66.0±1.6			<i>I</i>	2.13±0.30	77.4±4.0	
T	111613	DS Cru	<i>U</i>	2.55±0.07	86.3±0.7	g	111838	<i>U</i>	1.59±0.19	71.3±3.4	
			<i>B</i>	2.92±0.02	83.0±0.2			<i>B</i>	1.70±0.08	69.9±1.3	
			<i>V</i>	3.17±0.02	82.7±0.2			<i>V</i>	1.77±0.05	70.9±0.8	
			<i>R</i>	3.02±0.02	83.2±0.2			<i>R</i>	1.96±0.05	68.0±0.7	
			<i>I</i>	2.66±0.02	82.3±0.3			<i>I</i>	1.77±0.11	65.3±1.8	
U	111463		<i>U</i>	1.34±0.18	68.2±3.8	i	111886	<i>U</i>	1.62±0.16	77.2±3.8	
			<i>B</i>	1.66±0.14	68.1±2.4			<i>B</i>	2.03±0.17	87.4±1.2	
			<i>V</i>	1.61±0.08	66.7±1.4			<i>V</i>	2.43±0.08	85.2±0.5	
			<i>R</i>	1.66±0.08	68.7±1.4			<i>R</i>	2.33±0.10	84.7±0.6	
			<i>I</i>	1.59±0.16	66.9±2.9			<i>I</i>	1.87±0.18	82.3±1.5	
V	111916		<i>U</i>	2.82±0.10	79.2±1.1	k	111952	<i>U</i>	1.65±0.15	78.0±2.1	
			<i>B</i>	3.31±0.12	79.8±1.0			<i>B</i>	2.13±0.14	81.9±0.1	
			<i>V</i>	3.11±0.08	80.7±0.8			<i>V</i>	2.23±0.11	85.5±0.5	
			<i>R</i>	3.07±0.07	78.4±0.6			<i>R</i>	2.14±0.07	83.1±0.5	
			<i>I</i>	2.77±0.14	79.7±1.5			<i>I</i>	2.08±0.15	86.4±1.3	

TABLE 2 (CONTINUED)

Star <sup>a</sup>	HD/CPD <sup>b</sup>	GCVS/ <sup>c</sup> NSVS	Filter	$P_{\lambda} \pm \epsilon_P$ %	$\theta_{\lambda} \pm \epsilon_{\theta}$ °	Star <sup>a</sup>	HD/CPD <sup>b</sup>	GCVS/ <sup>c</sup> NSVS	Filter	$P_{\lambda} \pm \epsilon_P$ %	$\theta_{\lambda} \pm \epsilon_{\theta}$ °
a	111505	ET Cru	<i>U</i>	2.19±0.06	78.4±0.8	l	112026		<i>U</i>	1.78±0.04	85.3±0.6
			<i>B</i>	2.50±0.03	78.7±0.3				<i>B</i>	2.02±0.04	83.7±0.5
			<i>V</i>	2.67±0.04	78.1±0.4				<i>V</i>	2.03±0.03	86.0±0.4
			<i>R</i>	2.60±0.02	78.8±0.3				<i>R</i>	2.06±0.07	83.4±0.9
			<i>I</i>	2.27±0.03	78.8±0.3				<i>I</i>	1.66±0.08	81.5±1.3
b	111656		<i>U</i>	2.17±0.13	75.5±1.8	m	112027		<i>U</i>	1.63±0.13	54.6±2.3
			<i>B</i>	2.66±0.15	75.4±1.6				<i>B</i>	2.17±0.14	54.2±0.4
			<i>V</i>	2.72±0.09	74.9±1.0				<i>V</i>	2.54±0.10	46.0±0.3
			<i>R</i>	2.75±0.10	73.3±1.0				<i>R</i>	2.61±0.09	45.4±0.3
			<i>I</i>	2.25±0.21	78.3±2.6				<i>I</i>	2.42±0.14	42.8±0.6
d	111699		<i>U</i>	1.81±0.13	79.1±2.0	n	112168		<i>U</i>	1.90±0.10	72.9±1.5
			<i>B</i>	2.38±0.14	78.4±1.7				<i>B</i>	2.19±0.03	73.1±0.4
			<i>V</i>	2.16±0.09	79.8±1.2				<i>V</i>	2.33±0.03	72.5±0.3
			<i>R</i>	2.04±0.09	76.9±1.3				<i>R</i>	2.30±0.03	74.1±0.4
			<i>I</i>	2.02±0.20	76.2±2.8				<i>I</i>	2.08±0.02	72.2±0.3
e	111714	19503	<i>U</i>	2.46±0.19	78.8±2.2	p	112181		<i>U</i>	1.71±0.08	79.2±1.4
			<i>B</i>	2.98±0.11	74.6±1.1				<i>B</i>	2.01±0.03	82.4±0.4
			<i>V</i>	2.93±0.09	76.4±0.8				<i>V</i>	2.21±0.03	82.7±0.4
			<i>R</i>	3.00±0.07	74.5±0.7				<i>R</i>	2.18±0.02	82.7±0.3
			<i>I</i>	2.27±0.15	77.4±1.9				<i>I</i>	1.78±0.03	81.9±0.4
105		BV Cru	<i>U</i>	2.55±0.05	76.2±0.5	138	-59°4536		<i>U</i>	2.35±0.28	83.0±3.4
			<i>B</i>	2.64±0.02	75.9±0.2				<i>B</i>	2.29±0.12	78.1±1.6
			<i>V</i>	2.77±0.02	76.5±0.2				<i>V</i>	2.69±0.09	77.0±0.9
			<i>R</i>	2.64±0.02	75.0±0.2				<i>R</i>	2.92±0.09	73.5±0.9
			<i>I</i>	2.37±0.04	72.3±0.5				<i>I</i>	2.51±0.17	74.0±1.9
106	111934	BU Cru	<i>U</i>	2.51±0.09	78.1±1.1	139			<i>U</i>	1.82±0.23	81.0±3.6
			<i>B</i>	2.98±0.04	77.6±0.4				<i>B</i>	3.26±0.15	79.6±1.3
			<i>V</i>	2.93±0.03	75.7±0.3				<i>V</i>	2.81±0.11	81.1±1.2
			<i>R</i>	2.81±0.03	75.4±0.3				<i>R</i>	2.91±0.09	78.6±0.9
			<i>I</i>	2.53±0.04	76.3±0.4				<i>I</i>	2.68±0.20	75.9±2.1
107		CR Cru	<i>U</i>	2.54±0.17	70.6±2.0	201		EI Cru	<i>U</i>	1.57±0.10	81.8±1.8
			<i>B</i>	2.76±0.18	73.5±1.9				<i>B</i>	1.80±0.14	75.2±2.2
			<i>V</i>	2.86±0.09	73.9±0.9				<i>V</i>	1.83±0.11	77.8±1.7
			<i>R</i>	2.83±0.04	75.0±0.4				<i>R</i>	1.79±0.09	75.6±1.5
			<i>I</i>	2.72±0.06	75.5±0.7				<i>I</i>	1.66±0.18	74.6±3.2
113	-59°4532	19532	<i>U</i>	2.57±0.16	79.4±1.7	202	-59°4558	CX Cru	<i>U</i>	2.26±0.05	74.4±0.6
			<i>B</i>	2.64±0.04	72.0±0.5				<i>B</i>	2.49±0.06	73.0±0.7
			<i>V</i>	2.75±0.04	72.6±0.4				<i>V</i>	2.68±0.03	75.8±0.3
			<i>R</i>	2.78±0.04	70.3±0.4				<i>R</i>	2.85±0.02	74.8±0.2
			<i>I</i>	2.49±0.06	69.9±0.7				<i>I</i>	2.80±0.02	74.2±0.2
115	-59°4541		<i>U</i>	2.40±0.13	75.2±1.6	203	-59°4556		<i>U</i>	2.50±0.08	72.8±0.9
			<i>B</i>	2.57±0.05	71.9±0.6				<i>B</i>	2.84±0.04	75.4±0.4
			<i>V</i>	2.77±0.06	75.5±0.6				<i>V</i>	2.74±0.03	74.7±0.3
			<i>R</i>	2.56±0.05	74.8±0.5				<i>R</i>	2.99±0.03	74.7±0.3
			<i>I</i>	2.44±0.09	72.8±1.0				<i>I</i>	2.92±0.02	73.9±0.2
116		EE Cru	<i>U</i>	2.68±0.30	79.4±3.1	207			<i>U</i>	2.60±0.94	71.9±10.0
			<i>B</i>	2.37±0.15	74.3±1.8				<i>B</i>	2.08±0.20	72.9±2.7
			<i>V</i>	2.77±0.13	75.7±1.3				<i>V</i>	2.75±0.25	70.5±2.6
			<i>R</i>	2.76±0.07	73.2±0.8				<i>R</i>	3.01±0.16	67.5±1.5
			<i>I</i>	2.30±0.16	72.8±2.0				<i>I</i>	2.28±0.49	71.0±6.1
117	-59°4531		<i>U</i>	2.54±0.11	70.0±1.2	215		EH Cru	<i>U</i>	2.12±0.18	72.5±2.4
			<i>B</i>	2.84±0.04	71.1±0.4				<i>B</i>	2.77±0.05	70.2±0.5
			<i>V</i>	3.11±0.03	70.7±0.3				<i>V</i>	3.10±0.05	72.8±0.5
			<i>R</i>	2.98±0.05	70.5±0.5				<i>R</i>	3.10±0.05	72.4±0.5
			<i>I</i>	2.76±0.04	69.7±0.4				<i>I</i>	2.63±0.06	74.3±0.7
137			<i>U</i>	2.27±0.18	83.5±2.2	216			<i>U</i>	2.92±0.37	68.7±3.6
			<i>B</i>	2.69±0.25	79.8±2.6				<i>B</i>	3.03±0.09	73.0±0.8
			<i>V</i>	2.64±0.12	78.6±1.3				<i>V</i>	3.11±0.08	76.5±0.8
			<i>R</i>	2.80±0.16	77.8±1.6				<i>R</i>	2.79±0.11	72.6±1.1
			<i>I</i>	1.41±0.31	75.2±6.1				<i>I</i>	2.51±0.10	74.1±1.1

TABLE 2 (CONTINUED)

Star <sup>a</sup>	HD/CPD <sup>b</sup>	GCVS/ <sup>c</sup> NSVS	Filter	$P_{\lambda} \pm \epsilon_P$ %	$\theta_{\lambda} \pm \epsilon_{\theta}$ °	Star <sup>a</sup>	HD/CPD <sup>b</sup>	GCVS/ <sup>c</sup> NSVS	Filter	$P_{\lambda} \pm \epsilon_P$ %	$\theta_{\lambda} \pm \epsilon_{\theta}$ °
218			<i>U</i>	1.24±0.41	80.2±9.2	306	-59° 4559	CW Cru	<i>U</i>	2.16±0.08	83.5±1.1
			<i>B</i>	1.67±0.16	73.8±2.7				<i>B</i>	2.24±0.05	87.1±0.7
			<i>V</i>	1.77±0.06	79.6±1.0				<i>V</i>	2.57±0.05	83.9±0.6
			<i>R</i>	1.61±0.08	77.4±1.4				<i>R</i>	2.60±0.05	81.8±0.5
			<i>I</i>	1.53±0.17	75.2±3.2				<i>I</i>	2.21±0.07	83.1±0.9
222			<i>U</i>	2.82±0.43	64.1±4.3	307	-59° 4560	CY Cru	<i>U</i>	1.67±0.19	78.1±3.2
			<i>B</i>	3.02±0.16	78.7±1.5				<i>B</i>	2.67±0.12	77.2±1.3
			<i>V</i>	2.84±0.08	77.6±0.8				<i>V</i>	2.43±0.08	78.4±1.0
			<i>R</i>	2.61±0.10	73.5±1.1				<i>R</i>	2.46±0.21	73.8±2.5
			<i>I</i>	2.42±0.17	76.7±2.0				<i>I</i>	1.62±0.18	71.5±3.1
223	-59° 4551	CC Cru	<i>U</i>	2.34±0.70	87.2±8.3	311	-59° 4565		<i>U</i>	1.87±0.09	76.8±1.3
			<i>B</i>	2.97±0.15	75.4±1.4				<i>B</i>	2.31±0.16	78.6±1.9
			<i>V</i>	3.25±0.13	76.0±1.1				<i>V</i>	2.57±0.06	77.4±0.7
			<i>R</i>	3.15±0.11	75.4±1.0				<i>R</i>	2.43±0.07	76.4±0.8
			<i>I</i>	2.86±0.16	73.1±1.6				<i>I</i>	2.44±0.14	78.5±1.7
224			<i>U</i>	2.56±0.11	83.5±1.2	405	-59° 4544	EF Cru	<i>U</i>	2.59±0.12	75.8±1.3
			<i>B</i>	3.20±0.04	77.3±0.4				<i>B</i>	2.44±0.05	75.9±0.6
			<i>V</i>	3.43±0.03	76.3±0.3				<i>V</i>	2.75±0.04	74.1±0.4
			<i>R</i>	3.31±0.04	76.7±0.4				<i>R</i>	2.52±0.05	74.6±0.6
			<i>I</i>	2.92±0.04	77.0±0.4				<i>I</i>	2.33±0.07	73.9±0.9
228	-59° 4571		<i>U</i>	2.44±0.14	80.3±1.7	410	-59° 4533	19531	<i>U</i>	2.73±0.12	62.5±1.2
			<i>B</i>	2.80±0.11	77.7±1.1				<i>B</i>	2.71±0.07	72.6±0.7
			<i>V</i>	2.71±0.07	77.2±0.7				<i>V</i>	2.71±0.03	70.7±0.3
			<i>R</i>	2.95±0.08	75.2±0.7				<i>R</i>	2.68±0.06	69.0±0.6
			<i>I</i>	2.75±0.24	72.6±2.4				<i>I</i>	2.44±0.07	67.0±0.9
229			<i>U</i>	...	...	414	-59° 4535		<i>U</i>	1.45±0.86	155.6±15.3
			<i>B</i>	3.81±0.60	63.6±4.4				<i>B</i>	2.20±0.12	77.3±1.6
			<i>V</i>	2.44±0.42	76.1±0.3				<i>V</i>	2.63±0.05	74.5±0.5
			<i>R</i>	3.08±0.44	81.2±1.3				<i>R</i>	2.76±0.05	71.3±0.5
			<i>I</i>	2.36±0.15	76.2±1.0				<i>I</i>	2.40±0.11	69.6±1.2
301	-59° 4549	CT Cru	<i>U</i>	2.16±0.13	71.7±1.7	417	-59° 4546	CS Cru	<i>U</i>	1.71±0.15	80.2±2.5
			<i>B</i>	2.53±0.06	75.9±0.7				<i>B</i>	2.23±0.13	83.0±1.7
			<i>V</i>	2.69±0.03	76.2±0.3				<i>V</i>	2.47±0.05	84.0±0.6
			<i>R</i>	2.69±0.05	76.6±0.6				<i>R</i>	2.42±0.06	86.0±0.8
			<i>I</i>	2.34±0.06	72.6±0.8				<i>I</i>	2.55±0.04	84.3±0.4
305	-59° 4557	CN Cru	<i>U</i>	2.38±0.03	73.1±0.3	418	-59° 4542	BT Cru	<i>U</i>	2.12±0.15	77.9±2.0
			<i>B</i>	2.69±0.02	73.3±0.2				<i>B</i>	2.34±0.10	74.8±1.2
			<i>V</i>	2.90±0.03	73.7±0.2				<i>V</i>	2.84±0.04	77.1±0.4
			<i>R</i>	2.98±0.03	71.9±0.3				<i>R</i>	2.56±0.04	77.0±0.4
			<i>I</i>	2.61±0.03	72.6±0.4				<i>I</i>	3.11±0.03	76.6±0.3
423			<i>U</i>	2.07±0.87	96.9±11.3	424			<i>U</i>	3.87±0.49	83.8±3.6
			<i>B</i>	2.48±0.20	73.1±2.3				<i>B</i>	2.43±0.22	77.1±2.5
			<i>V</i>	2.86±0.16	66.5±1.6				<i>V</i>	3.37±0.14	71.6±1.2
			<i>R</i>	3.02±0.14	72.8±1.3				<i>R</i>	2.82±0.10	68.8±1.0
			<i>I</i>	2.56±0.22	70.5±2.5				<i>I</i>	3.07±0.18	68.8±1.7

<sup>a</sup>(Arp & van Sant 1958; capital letters); (Dachs & Kaiser 1984; small letters and modifications according to the text).

<sup>b</sup>Henry Draper or Cape Photographic Durchmusterung identification.

<sup>c</sup>General Catalog of Variable Stars, Kholopov 1998 (II/214A) or New Catalog of Suspected Variable Stars Supplement, Kazarovets 1998 (II/219).

parameter (the unit weight error of the fit; Marraco et al. 1993) in order to quantify the departure of our data from the “theoretical curve” of Serkowski’s law. In our scheme, when a star exhibits  $\sigma_1 > 1.70$  (empirical limit) it indicates the presence of intrinsic stellar polarization, that is, polarization of a non-interstellar origin as part of the measured polarization. There is a second criterion to identify intrinsic polarization: the individual  $\lambda_{max}$  values. Stars with

much shorter  $\lambda_{max}$  than the average value for the interstellar medium (0.55  $\mu\text{m}$ ; Serkowski et al. 1975) are candidates to have an intrinsic component of polarization as well (Orsatti et al. 1998). In Table 3, the calculated value of the  $\sigma_1$  parameter for each star is listed in Column (3), while Column (5) shows the intrinsic polarization criterion used to detect it. The mathematical expression of the  $\sigma_1$  parameter is also shown as a footnote.

TABLE 3  
POLARIZATION RESULTS OF STARS IN NGC 4755

Star <sup>a</sup>	$P_{\max} \pm \epsilon_p$ %	$\sigma_1^b$	$\lambda_{\max} \pm \epsilon_\lambda$ $\mu\text{m}$	Intr.pol. criteria	Sp. T. <sup>c</sup>	Memb. <sup>d</sup>	This work
A	$3.00 \pm 0.02$	1.20	$0.54 \pm 0.01$		B9 Ia (1)	m:	nm
B	$2.49 \pm 0.07$	2.02	$0.57 \pm 0.03$	$\sigma_1$	B3 Ia (1)	m	nm
C	$3.23 \pm 0.10$	1.33	$0.60 \pm 0.03$		B2 III (1)	m:	nm
D	$2.75 \pm 0.02$	1.19	$0.58 \pm 0.01$		M2 Iab (2)	m	nm
E	$2.78 \pm 0.04$	2.74	$0.57 \pm 0.01$	$\sigma_1$	B1 III (1)	m	member
F	$2.69 \pm 0.09$	1.73	$0.55 \pm 0.04$	$\sigma_1$	$\beta$ Cephei var.(*)	m:	member
G	$2.79 \pm 0.03$	1.41	$0.56 \pm 0.01$		$\beta$ Cephei var.(*)	m	member
H	$2.47 \pm 0.11$	1.32	$0.58 \pm 0.04$		B1.5 Vne (1)	m	nm
I	$3.39 \pm 0.07$	1.68	$0.59 \pm 0.02$		$\beta$ Cephei var.(*)	m	nm
J	$2.50 \pm 0.03$	1.09	$0.56 \pm 0.01$		B2 V (1)	m	nm
K	$2.91 \pm 0.05$	1.04	$0.50 \pm 0.01$		B3 V (1)	m:	member
L	$2.81 \pm 0.05$	1.02	$0.60 \pm 0.02$		B8 V (3)	m	member
M	$3.22 \pm 0.16$	1.71	$0.51 \pm 0.04$		B8 III-V (1)	m:	nm
N	$2.09 \pm 0.07$	0.34	$0.43 \pm 0.02$	$\lambda_{\max}$	...	nm	nm
O	$2.57 \pm 0.11$	1.71	$0.56 \pm 0.04$		...	nm	nm
P	$2.94 \pm 0.08$	1.43	$0.57 \pm 0.03$		...	m	nm
Q	$2.37 \pm 0.21$	1.53	$0.45 \pm 0.06$	$\lambda_{\max}$	...	nm	nm
T	$3.12 \pm 0.02$	1.28	$0.55 \pm 0.01$		A2 Iabe (4)	m:	...
U	$1.70 \pm 0.04$	0.83	$0.59 \pm 0.03$		A3 II (5)	nm	...
V	$3.27 \pm 0.07$	1.59	$0.53 \pm 0.02$		B1 V (5)	m	...
a	$2.66 \pm 0.00$	0.18	$0.55 \pm 0.00$		B2-3 III (6)	m:	...
b	$2.77 \pm 0.03$	0.56	$0.57 \pm 0.01$		B3 III (5)	m:	...
d	$2.22 \pm 0.07$	1.41	$0.54 \pm 0.03$		B2-3 III (5)	m:	...
e	$3.04 \pm 0.07$	1.40	$0.54 \pm 0.02$		B2-3 II-III (5)	m:	poss.member
f	$2.19 \pm 0.06$	0.89	$0.54 \pm 0.03$		B1-3 Vnn (5)	nm	...
g	$1.92 \pm 0.05$	1.39	$0.63 \pm 0.04$		B8 (5)	nm	...
i	$2.35 \pm 0.08$	1.20	$0.60 \pm 0.04$		B3 IV (5)	nm	...
k	$2.23 \pm 0.04$	0.85	$0.59 \pm 0.02$		B1 III (7)	nm	...
l	$2.08 \pm 0.03$	1.31	$0.53 \pm 0.01$		B0.5 IV (5)	nm	...
m	$2.62 \pm 0.04$	0.59	$0.67 \pm 0.01$		B1 II V (8)	nm	...
n	$2.36 \pm 0.01$	0.74	$0.57 \pm 0.00$		B9 V (5)	nm	...
p	$2.17 \pm 0.04$	2.48	$0.55 \pm 0.02$	$\sigma_1$	B2-3 II-III (5)	m:	...
105	$2.78 \pm 0.03$	2.55	$0.53 \pm 0.01$	$\sigma_1$	$\beta$ Cephei var.(*)	m	member
106	$2.99 \pm 0.05$	2.49	$0.53 \pm 0.02$	$\sigma_1$	B1.5 Ib (1)	m	member:
107	$2.91 \pm 0.06$	1.71	$0.58 \pm 0.03$		B5 V (1)	m:	member:
113	$2.82 \pm 0.03$	1.49	$0.56 \pm 0.01$		$\beta$ Cephei var.(*)	m	poss.member
115	$2.72 \pm 0.05$	1.53	$0.54 \pm 0.02$		B1 V (3)	m	member
116	$2.77 \pm 0.08$	1.27	$0.56 \pm 0.04$		A0 II (1)	m:	member
117	$3.10 \pm 0.02$	1.19	$0.57 \pm 0.01$		B2.5 Vn (1)	m:	nm
137	$2.68 \pm 0.17$	1.72	$0.50 \pm 0.06$		B6-7 III (1)	m:	poss.member
138	$2.83 \pm 0.09$	1.27	$0.64 \pm 0.04$		B2 V (1)	m	member



TABLE 3 (CONTINUED)

Star <sup>a</sup>	$P_{\max} \pm \epsilon_p$ %	$\sigma_1$ <sup>b</sup>	$\lambda_{\max} \pm \epsilon_\lambda$ $\mu\text{m}$	Intr.pol. criteria	Sp. T. <sup>c</sup>	Memb. <sup>d</sup>	This work
139	$2.98 \pm 0.17$	2.54	$0.59 \pm 0.07$	$\sigma_1$	B3 Vn (1)	m	nm
201	$1.89 \pm 0.03$	0.49	$0.55 \pm 0.01$		$\beta$ Cephei var. (*)	m:	nm
202	$2.89 \pm 0.07$	4.80	$0.63 \pm 0.03$	$\sigma_1$	$\beta$ Cephei var. (*)	m	member
203	$3.05 \pm 0.10$	6.59	$0.62 \pm 0.04$	$\sigma_1$	B1 V (3)	m	member
207	$2.93 \pm 0.23$	1.08	$0.72 \pm 0.08$		B3 Vn (1)	m	nm
215	$3.06 \pm 0.05$	1.63	$0.58 \pm 0.02$		B3 V (1)	m	nm
216	$3.11 \pm 0.05$	0.83	$0.51 \pm 0.01$		B5 V (1)	m	nm
218	$1.74 \pm 0.04$	0.69	$0.54 \pm 0.03$		B3 V (1)	m:	nm
222	$2.91 \pm 0.09$	1.04	$0.49 \pm 0.03$		Be (9)	m	member
223	$3.25 \pm 0.02$	0.33	$0.58 \pm 0.01$		B2 III (1)	m	nm
224	$3.40 \pm 0.03$	1.38	$0.56 \pm 0.01$		B0 V (3)	m:	nm
228	$2.92 \pm 0.10$	2.06	$0.58 \pm 0.04$	$\sigma_1$	B8 (10)	m	member
229	$3.03 \pm 0.44$	1.48	$0.52 \pm 0.08$		B7 (4)	nm	nm
301	$2.70 \pm 0.01$	0.56	$0.56 \pm 0.01$		$\beta$ Cephei var. (*)	m	member
305	$2.95 \pm 0.03$	1.91	$0.57 \pm 0.01$	$\sigma_1$	B1 V (1)	m:	member:
306	$2.57 \pm 0.05$	1.72	$0.57 \pm 0.02$		B2 IV ne (2)	m	nm
307	$2.43 \pm 0.15$	2.17	$0.50 \pm 0.06$	$\sigma_1$	$\beta$ Cephei var. (*)	m	m:
311	$2.56 \pm 0.05$	1.22	$0.60 \pm 0.02$		B2 V (3)	m:	member:
405	$2.69 \pm 0.07$	2.56	$0.54 \pm 0.03$	$\sigma_1$	$\beta$ Cephei var. (*)	m	member
410	$2.78 \pm 0.07$	2.56	$0.53 \pm 0.03$	$\sigma_1$	B3 Ve (3)	m:	nm
414	$2.72 \pm 0.04$	1.02	$0.64 \pm 0.02$		B1 V (3)	m	member:
417	$2.59 \pm 0.05$	1.76	$0.68 \pm 0.03$	$\sigma_1$	B1.5e (1)	m	nm
418	$2.99 \pm 0.17$	6.89	$0.73 \pm 0.08$	$\sigma_1$	$\beta$ Cephei var. (*)	m	member
423	$2.92 \pm 0.06$	0.61	$0.62 \pm 0.03$		...	m	nm
424	$3.07 \pm 0.21$	2.90	$0.58 \pm 0.09$	$\sigma_1$	B8 III-V (1)	m	nm

<sup>a</sup>(Arp & van Sant 1958) (capital letters); (Dachs & Kaiser 1984) (small letters and modifications according to the text).

<sup>b</sup> $\sigma_1^2 = \sum (r_\lambda / \epsilon_{p_\lambda})^2 / (m - 2)$ ; where  $m$  is the number of colors and  $r_\lambda = P_\lambda - P_{\max} \exp(-K \ln^2(\lambda_{\max}/\lambda))$ .

<sup>c</sup>Sp. T. references: 1.- (Evans et al. 2005); 2.- (Schild 1970); 3.- (Feast 1963); 4.- (Hiltner et al. 1969); 5.- (Houck & Cowley 1975); 6.- Samus (GCVS); 7.- (Beer 1961); 8.- (Garrison et al. 1977); 9.- (McSwain & Gies 2005b); 10.- (Cannon & Mayall 1949). (\*) indicates Sp. T. in Table 3.

<sup>d</sup>(Dachs & Kaiser 1984).

From the results, it can be seen that about one third (19 out of 66) of the observed stars display features of intrinsic polarization in their light smaller than those we found in the open cluster NGC 6611: 50% in the core (Orsatti et al. 2000) and 47% in the halo (Orsatti et al. 2006), but still very important. It is known that there is a great number of variable stars present in NGC 4755, which could be the origin of intrinsic polarization in some cases. There are, for example,  $\beta$  Cephei stars whose polarimetric charac-

teristics will be studied in the following subsection. Excluding these variables, the possible origins of the polarization in the stars selected through the first criterion may be: (1) scattering in circumstellar material due to evolution (stars #B, #E, #p, #424); (2) scattering in extended atmospheres of Be stars: #410, #417; (3) binarity: #106, an ellipsoidal variable (Jakate 1978); #305, an eclipsing binary of the Lyra type (semi-detached; Jakate 1978); (4) possible binarity: #139 (McSwain et al. 2009). We do not

know why #203 ( $\sigma_1 = 6.59$ ; B1 V) and # 228 (B8 V) display features of intrinsic polarization. The second criterion, selects two stars: N ( $\lambda_{max} = 0.43\mu\text{m}$ ) and Q ( $\lambda_{max} = 0.45\mu\text{m}$ ); there is no information on them in the literature.

#### 4.2. $\beta$ Cephei stars in NGC 4755

Table 4 contains information on eleven  $\beta$  Cephei observed in NGC 4755. For six of them, that is, for about half of variables, the value of the  $\sigma_1$  parameter is larger than 1.70, which indicates the presence of intrinsic polarization in the light. Since a radial pulsation does not cause linear polarization and a non-radial oscillation would cause a periodic and very small intrinsic polarization, we think it could be of interest to find possible origins of this polarization: light scattering within a dust envelope or in an extended atmosphere, within the outer envelope of some binary systems, or more than one mechanism. In Figure 3 we plot the polarization and position angle dependence with the wavelength of these stars, while Figure 4 shows similar plots for the variables not affected by intrinsic polarization, according to the  $\sigma_1$  parameter. In both of them, the solid curve denotes the Serkowski polarization relation for the interstellar medium; the value of the  $\sigma_1$  parameter is shown for each star.

The main characteristics present in the  $P_V$  vs.  $\lambda$  curves are listed below.

**4755-F:** B1 V - B2 II-III. A strong rotation of the  $\theta_U$  value and  $P_U$  above the Serkowski curve can be seen, while the rest of the polarizations adjust quite well. Both facts suggest a mechanism of light scattering in an extended atmosphere. In this case, the star must be an evolved one (as classified by Hernandez 1960, Feast 1963 or Schild 1970; Table 4) and not a main sequence star (Evans et al. 2005; same table).

**4755-105:** B0.5 V - B1 II-III<sub>n</sub>.  $P_U$  is slightly above the Serkowski curve, and the rest of the measures fit well. Strong rotations in  $\theta_R$  and  $\theta_I$  can be seen. There are indications of diffuse lines in the spectra, indicating possible binarity.

**4755-202:** B1 V - B2 IV. A very high  $\sigma_1 = 4.80$ . Rotation in  $\theta_U$  and  $\theta_B$  polarization angles can be seen.

**4755-307:** B1.5 V. Even considering the observational errors, the  $\theta_\lambda$  curve resembles that of #105. (Evans et al. 2005) has proposed the star as a potential binary, in view of variations in the  $V_r$  measures.

**4755-405:** B2 V. The origin of the intrinsic polarization is unclear; there is no rotation of the  $\theta$  angles.

**4755-418:** B2 V-III.  $P_U$  is above the standard curve, suggesting light scattering in an extended atmosphere. The  $\sigma_1$  value, which amounts to 6.89, is very high. The star has been proposed as a potential binary by (Evans et al. 2005).

For the rest of the variables,  $\sigma_1$  is below the empirical limit. Their curves (Figure 4) show a good fit to the Serkowski curve; the exception is #113, whose plot resembles that of #202, even though the  $\sigma_1$  parameter is below 1.70 in this case.

#### 4.3. The $Q_V$ vs. $U_V$ tool for membership assignment

The plot of the Stokes parameters  $Q_V$  vs.  $U_V$  for the V-bandpass, where  $Q_V = P_V \cos(2\theta_V)$  and  $U_V = P_V \sin(2\theta_V)$  are components in the equatorial system of the polarization vector  $P_V$ , is an important polarimetric tool that illustrates the variations occurring in interstellar environments. Since the light from cluster members must have traversed a common sheet of dust of particular polarimetric characteristics, the member data points should occupy similar regions of the plot. Non-member (frontside and background) stars should be located somewhat apart from the region occupied by member stars, since their light must have traveled through dust clouds that are different from those affecting the light of member stars, with different polarimetric characteristics. The polarimetric observations constitute an excellent tool to determine memberships, in particular when field stars have colors similar to those of cluster members (see, e.g. Orsatti et al. 2010).

Figure 5 shows the plot of the observed stars, where the point of coordinates  $Q_V = 0$  and  $U_V = 0$  indicates the dustless solar neighborhood, and the others represent the direction of the polarization vector  $P_V$  as seen from the Sun. Fifteen stars located far from the central part of NGC 4755 are shown with crosses (#T-U-V-a-b-d-e-f-g-i-k-l-m-n-p; see Figure 1b of Dachs & Kaiser 1984) and have been excluded from the analysis, since their individual positions in the plot would represent stellar environments different from those associated with the cluster itself. The point of coordinates  $Q_V = -2.5$ ,  $U_V = 1.4$  is surrounded by a group of seven stars: #K-L-115-116-138-222-311, all of them with no indications of intrinsic polarization. For the group, we obtained mean values  $P_V = 2.76 \pm 0.13$  (%) and  $\theta_V = 76.6 \pm 0.9$  (both, mean of 7 stars) which we take as representative parameters of the interstellar medium at the cluster position. The wavelength of maximum polarization for the same group of stars amounts to  $0.56 \pm 0.04 \mu\text{m}$ , very similar to the mean

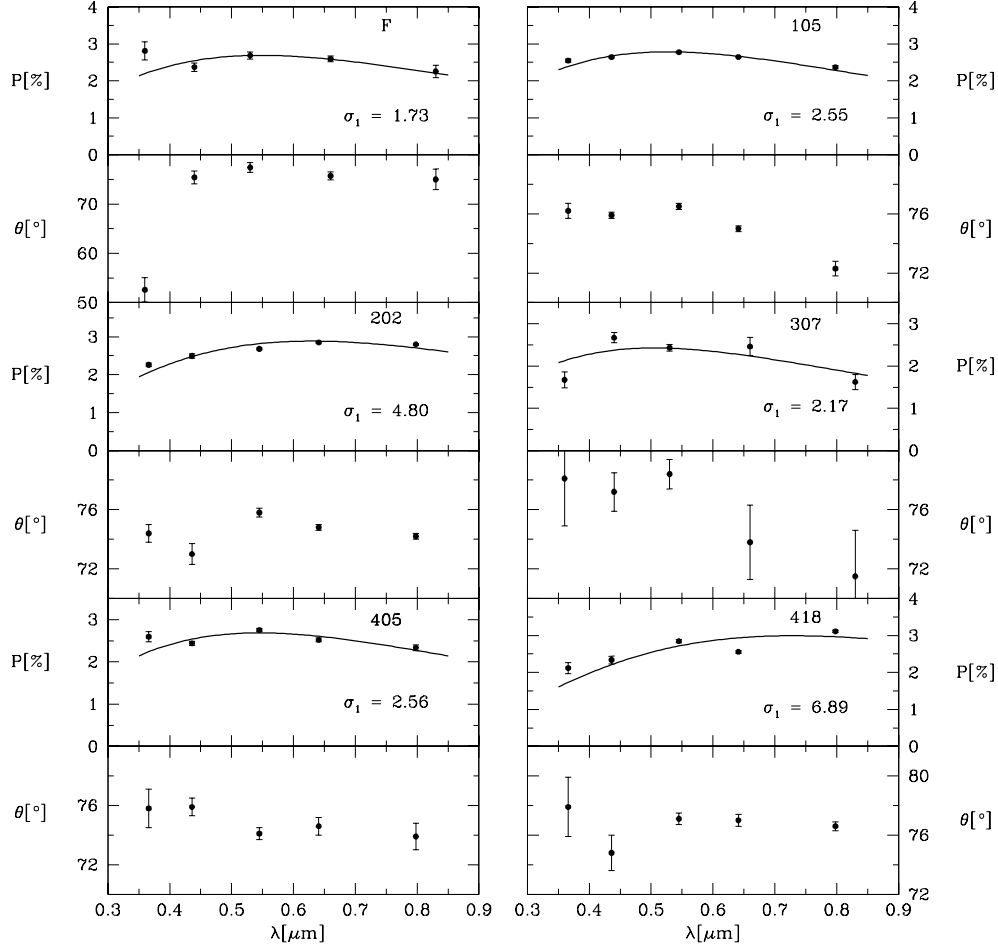


Fig. 3. The plot shows both the polarization and position angle dependence on wavelength, of the  $\beta$  Cephei with indications of intrinsic polarization, where the solid curve denotes the Serkowski polarization relation for the general interstellar medium (ISM). The value of the  $\sigma_1$  parameter is also shown.

value for the ISM:  $\lambda_{max} = 0.545 \mu\text{m}$  (Serkowski et al. 1975). Now, we have identified as members of the cluster those stars with  $P \pm 1\sigma$  and  $\theta \pm 1\sigma$ : stars #107, 137 (pm), 203, 228, 305, and 414 (pm), all of them without intrinsic polarization. The 13 members are shown in Figure 5 with filled circles.

The use of this method with stars showing intrinsic polarization is not straightforward, since some of them may get plotted inside the box only due to the possible modifications of  $P_v$  and  $\theta_v$ . For this reason, we added the membership information from (Dachs & Kaiser 1984) to the box approach. As a result, we identified three members (#E, 203 and 228) and two possible members (#106 and 305), all of them with intrinsic polarization. They are plotted with filled triangles.

The  $\beta$  Cephei variables (open squares) show preferences for open clusters (Stankov & Handler 2005); NGC 4755 and NGC 3293 are the objects with the

highest numbers. The variables we observed are seen in this figure in the membership region, with the exception of #I and #201, affected by very different interstellar mediums; and #307, all of them doubtful members.

In the last column of Table 3, we list our membership assignments, and those of (Dachs & Kaiser 1984) for the stars in common, in order to compare results from two different tools: polarimetric and photometric. In the latter case, they used differences between individual color excesses (or distance moduli) and the cluster averages:  $E_{B-V} = 0.44$  and  $V_0 - M_V = 11.77$  mag, to distinguish between members and non-members. Our tools allow us to show that the light from about 22 stars (m: or m according to them) has traveled through dust clouds different from those affecting the light of member stars, due to the different polarimetric characteristics; here, we list them as non-

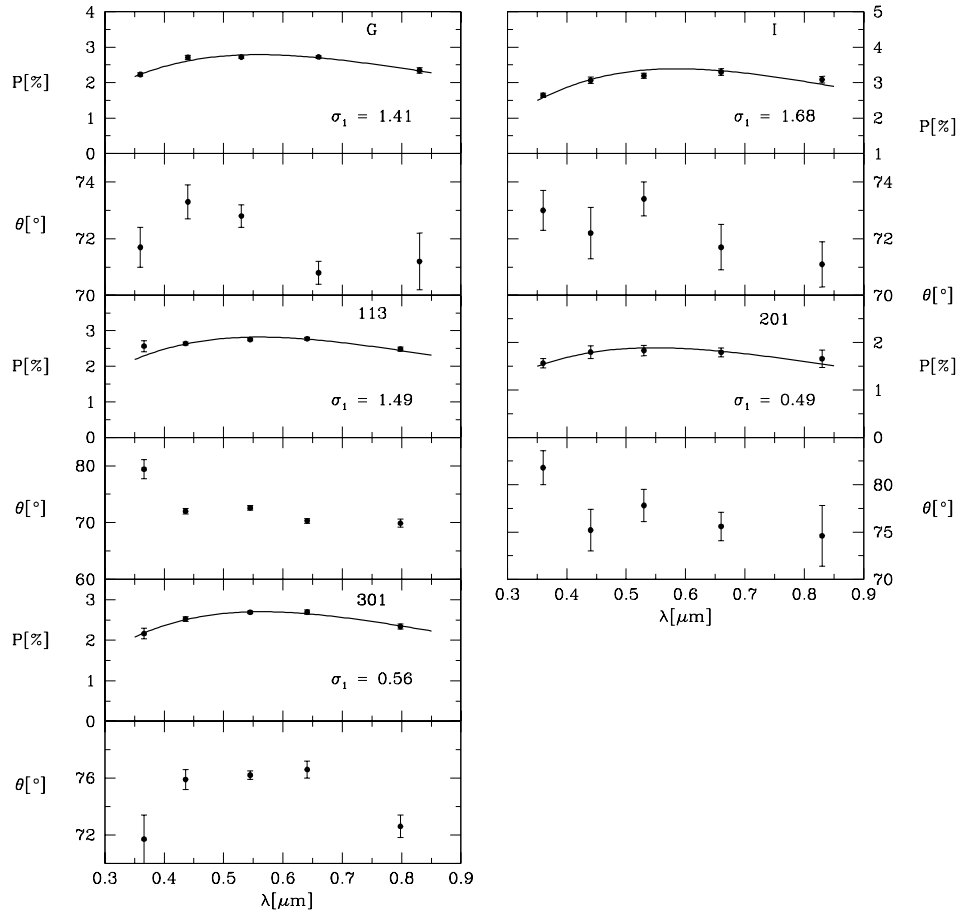


Fig. 4. Similar plots as in Figure 3 but for  $\beta$  Cephei without intrinsic polarization according to  $\sigma_1$ .

TABLE 4  
OBSERVED  $\beta$  CEPHEI STARS

Star	Identification GCVS/NSVS	Coordinates		$\sigma_1$	Sp. T.	References
		R.A.(2000)	Dec.(2000)			
F	BW Cru	12:53:57.5	-60:24:58.1	1.73	B0.5-1 II-III; B2III; B1 V	1, 2-3, 4
G	BS Cru	12:53:20.7	-60:23:16.9	1.41	B0.5 V; B1 V ; B1 III	2, 4, 5
I	CV Cru	12:53:46.9	-60:18:35.7	1.68	B1.5 Vn	2
105	BV Cru	12:53:39.2	-60:21:12.4	2.55	B1-2 II-III; B0.5 IIIIn; B0.5 V	1, 2, 4
113	19532	12:53:25.7	-60:22:00.2	1.49	B1 V; B2 IV	2, 5
201	EI Cru	12:53:52.0	-60:22:15.9	0.49	B1 V; B1 III	4, 5
202	CX Cru	12:53:51.7	-60:21:58.6	4.80	B1 V; B2 IV	2, 5
301	CT Cru	12:53:43.9	-60:22:29.4	0.56	B1.5 V	4
307	CY Cru	12:53:52.2	-60:22:27.9	2.17	B1.5 V	2, 3, 4
405	EF Cru	12:53:38.0	-60:22:39.6	2.56	B2 V	2, 3, 6
418	BT Cru	12:53:10.2	-60:25:59.6	6.89	B2 V; B1.5 V; B2 III	2, 4, 5

References: 1- Hernández 1960; 2- Feast 1963; 3- Schild 1970; 4- Evans et al. 2005; 5- Aidelman et al. 2012; 6- Stankov et al. 2002.

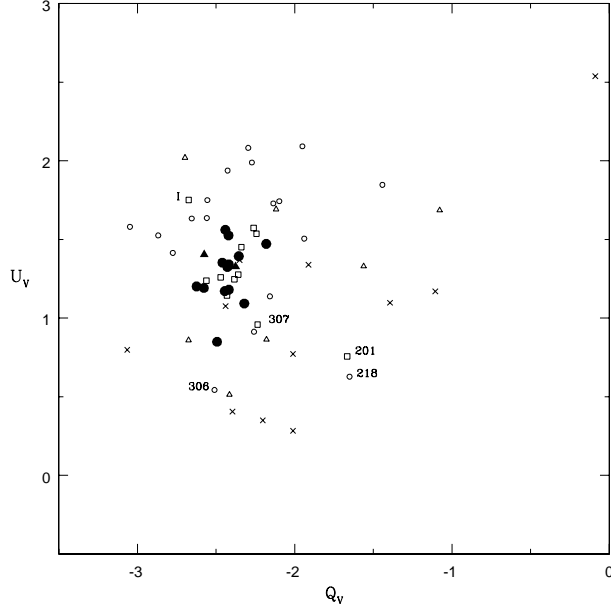


Fig. 5.  $Q_V$ - $U_V$  Stokes parameters for the observed stars. Filled and open circles are for members and non-members, respectively. Triangles are used for stars with intrinsic polarization according to Table 3; cross symbols show the position of stars located far from the cluster center. Finally, squares are used for  $\beta$  Cephei stars

members. In addition, we confirmed the membership (or possible membership) of another 22 stars, which shows the benefits of using the polarimetric tools.

#### 4.4. The $Q_V$ vs. $U_V$ plot as a tool to detect intrinsic polarization

Using methods different from the one described by (Poeckert et al. 1979) the  $(Q, U)$  plane can help us detect if at least part of the polarization measured in a star has an intrinsic origin. These methods try to separate the intrinsic (I) and the interstellar (IS) components of the measured polarization, by plotting the  $UBVRI$  polarization points of two stars: one of them affected only by interstellar polarization, and the other a target star. Two important assumptions must be made: (1) the interstellar polarization vector does not rotate with wavelength (Coyne 1974a); and (2) the polarization angle of the intrinsic polarization is independent of the wavelength. Assumption 2 is valid for Be stars (Capps et al. 1973, Coyne 1976), and also for some binary systems (Coyne & Kruszewski 1969, Capps et al. 1973, Poeckert 1975, etc.).

In a  $(Q, U)$  plot, the  $UBVRI$  polarization points of a star would all line up within the errors, with the best line going through  $(0,0)$  if there is only in-

TABLE 5  
OBSERVED AND INTERSTELLAR  
POLARIZATION

Star	$P_{max}$ %	$\lambda_{max}$ $\mu$ m	$P_{maxIS}$ %	$\theta_{IS}$ $^\circ$	$\theta_I$ $^\circ$	$\theta_{IS}-\theta_I$ $^\circ$
F	2.69	0.55	0.14	77.5	73.9	3.6
105	2.78	0.53	0.14	77.5	12.6	64.9
202	2.89	0.63	3.39	77.5	169.0	91.5
307	2.43	0.50	0.49	77.5	163.6	86.1
405	2.69	0.54	7.72	77.5	168.8	91.3
418	2.99	0.73	35.1	77.5	77.6	0.1

terstellar polarization. But in the same plot, the best line for a target star with features of intrinsic polarization would not pass through the origin, intersecting the former in a point  $(Q_0, U_0)$ , that would be the “head” of the interstellar polarization vector  $P_V$ ; the intrinsic polarization angle  $\theta_I$  is also obtained through the coordinates. The next step is to compute the IS polarization with Serkowski’s law, using  $P_{max}$  and adopting a  $\theta_{IS}$  evaluated from stars in the vicinity of the target star. Then, we have to subtract it from the observed polarization: the result is the intrinsic  $P_\lambda$ . According to this method, the fitting procedure will fail if the difference between  $\theta_{IS}$  and the resulting  $\theta_I$  is close to 0 or to 90 degrees.

We wanted to check if the intrinsic polarization detected in some of the  $\beta$  Cephei variables (§ 4.4) using the  $\sigma_1$  parameter, can be confirmed using Poeckert et al.’s method. To do this, we selected the  $UBVRI$  polarization data of #311 as representative of a star affected only by interstellar polarization and in the neighborhood of the target stars. It is located right in front of the variables and with no indications of intrinsic polarization. A simple average of the polarization angles in the  $UBVRI$  polarizations of the star gives  $\theta_{IS} = 77.5$  which we adopted as representative of the interstellar polarization angle. The best line through the origin was drawn using the  $UBVRI$  observations of the star. Next, we plotted the  $UBVRI$  observations of a target star and drew the best line as we did with #311.

Figure 6 shows the best lines for star #311 and for six variables in  $(Q, U)$  planes. Open and filled circles are used for the  $UBVRI$  observations of #311 and the variables, respectively. Table 5 lists the main results:  $P_{max}$  and  $\lambda_{max}$  from the observations, the interstellar value  $P_{max}(IS)$  and the adopted  $\theta_{IS}$ ; finally, the intrinsic polarization angle  $\theta_I$  and the dif-

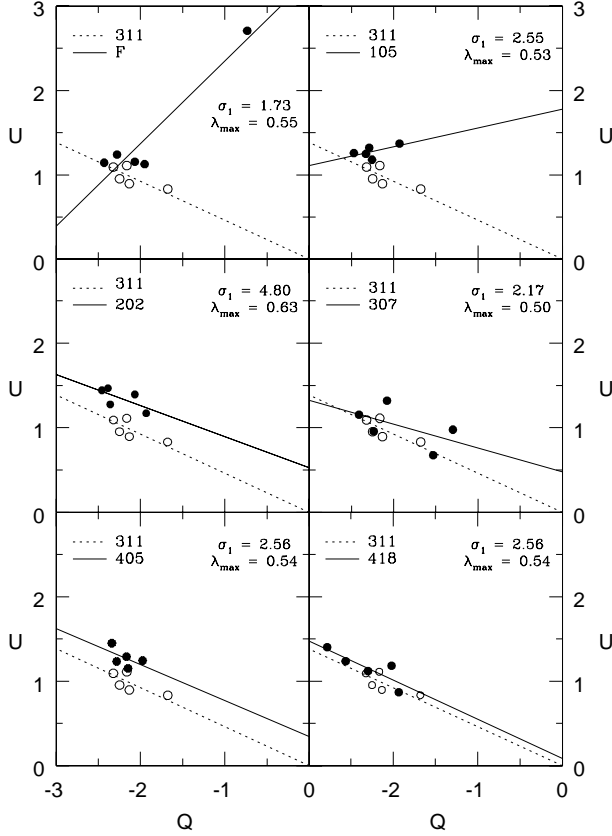


Fig. 6.  $UBVR$  data for star #311 (open symbols) and for  $\beta$  Cephei variables (filled symbols) in the  $(Q, U)$  plot.

ference between  $\theta_{IS}$  and  $\theta_I$ . The method fails for stars #202, #405, and #418 because their best lines are almost parallel to that for star #311. But for the rest (#F, #105, and #307), the difference in polarization angles points to an intrinsic origin in at least part of the polarization measured. We found that the contribution of the interstellar polarization  $P_{max}$  (IS) component is not significant to the polarization measured in these three stars.

#### 4.5. Polarization efficiency

It is supposed that the same dust that polarizes the light will redden it as well, and what is referred to as the polarization efficiency of the interstellar medium (ISM) (the ratio  $P_V/E_{B-V}$ ) is the degree of polarization produced for a given amount of reddening of the intervening dust grains. Assuming a normal interstellar material characterized by  $R_V = 3.1$ , the empirical upper limit relation for the polarization efficiency is given by:

$$P_V \leq 3 A_V \simeq 3 R_V E_{B-V} \quad (2)$$

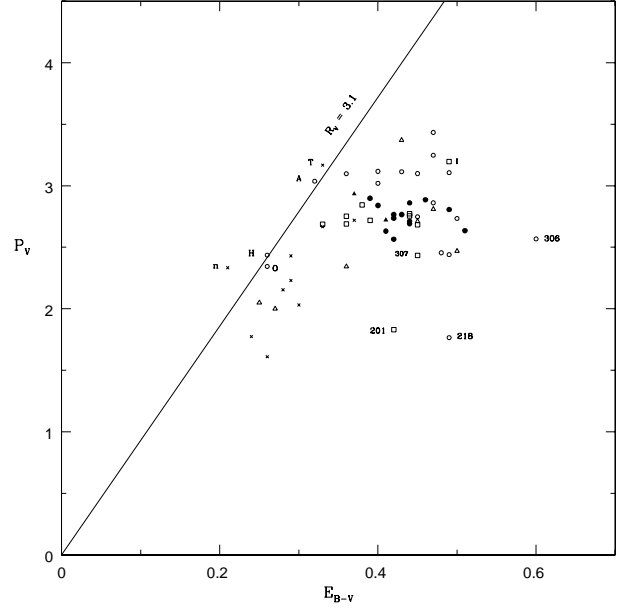


Fig. 7. Polarization efficiency diagram  $P_V$  vs.  $E_{B-V}$  for stars in the direction of NGC 4755. The line of the empirical maximum efficiency  $P_V = 9.3 E_{B-V}$  (solid line) is drawn adopting  $R_V = 3.1$ . Symbols are as in Figure 5.

(Serkowski et al. 1975). It provides a measure of the efficiency with which the grains are aligned. Nevertheless, other factors, such as the homogeneity of the magnetic field, the number of clouds in the line of sight (depolarizing the radiation due to different field directions), the cloud structure and the viewing angle with respect to the average magnetic field direction, will also influence the result. The polarization of stars that show values higher than  $P_V = 9 E_{B-V}$  can be immediately suspected to have a non-interstellar origin. Stars with lower values indicate that the alignment of dust grains is not total (or has multiple preferred orientations due to non-uniformity of the magnetic field along the line of sight), and/or that the grains are only moderately elongated particles (rather than infinite cylinders) that may be irregularly shaped.

Figure 7 shows the  $P_V$  vs.  $E_{B-V}$  plot for the observed stars; the solid line is the empirical upper limit obtained for interstellar dust particles adopting  $R_V = 3.1$ . Individual excesses were obtained either from the literature, dereddening the colors and using the relationship between spectral type and color indexes (Schmidt-Kaler 1982), or from the spectral type. In the figure, most of the observed stars lie on the right of the interstellar maximum efficiency line indicating that the observed polarization is in-

deed mostly due to the ISM. Even if it could have an intrinsic part, the resulting polarization gets plotted below the limit. Star #n has been classified as B8.5 Vn by (Garrison et al. 1977) and suspected of binarity. Star H is part of the visual binary IDS 12476S5952, and suspected of variability (Rufener & Bartholdi 1982); while #T and #A have spectral types A2 Iab and B9 Ia respectively; the origin of the intrinsic polarization may be in the evolutive state of both stars. The polarization efficiency for dust along the line of sight to NGC 4755 is higher than the mean: 6.3 vs. 5.0 for the general ISM. This implies that the alignment of the dust grains is very good.

The figure shows a grouping with excesses between 0.35 and 0.45 mag and polarizations in the range 2.5 to 3.0 %, whose stars would be cluster members. According to (Sagar & Cannon 1995), the differential reddening in NGC 4755 amounts to 0.05 mag, typical of a post-embedded young open cluster where molecular and dust clouds are dissipating. Polarimetrically, we found there is very little evidence for dust in the intracluster region.

At higher polarizations, there are some possible background stars, while at lower polarizations, say below  $P_V = 2.4\%$  approximately, there is a group of frontside stars. Three stars in the plot show evidences of a miscalculated  $E_{B-V}$ . One of them is #218, whose excess comes from the spectral type B3 V (Evans et al. 2005). The colors show some variations according to the WEBDA database; we think it could be an unresolved binary or that the luminosity class is wrong; star #306, classified as B2 IV ne (Schild 1970), also shows color variations in the database. Finally, #201 (EI Cru) is a  $\beta$  Cephei variable classified as B1 V (Evans et al. 2005) and B1 III (Aidelman et al. 2012). The intrinsic color  $(B - V)_0$  is -0.26 in both cases and the excess does not change with the spectral classification. The position in this figure shows it is not part of the cluster, as noted in the above subsection.

## 5. SUMMARY

We present *UBVRI* polarimetric observations of 66 stars in the direction of NGC 4755. A great number present intrinsic polarization, which in principle could be related to the fact that there are many different variables in the cluster, including eleven  $\beta$  Cephei. About half of them show features of intrinsic polarization in the light. Possible origins of these non-interstellar polarizations are found in the evolutive state (#F) and suspected binarity (#105-#307-#418); in addition, star #202 shows  $P_\lambda$  and

$\theta_\lambda$  curves which looks very similar to those of #418, and could be suspicious of binarity. A high number of binaries among the  $\beta$  Cephei in NGC 4755 is in accordance with the work of (Stankov & Handler 2005).

The polarization efficiency for dust along the line of sight to NGC 4755 is higher than the mean for the general ISM. This implies a very good alignment of the dust grains in direction of the cluster. The parameters of the interstellar medium at the cluster position are  $P_V = 2.76 \pm 0.13(\%)$  and  $\theta_V = 76^\circ.6 \pm 0^\circ.9$  (both of them, mean of 7 stars). The mean wavelength of maximum polarization amounts to  $0.56 \pm 0.04 \mu\text{m}$ , similar to the mean for the ISM ( $0.55 \mu\text{m}$ ). Using these values as representative of the dust in front of the cluster, a total of 25 stars were confirmed as members. In particular, three of the  $\beta$  Cephei were found to be doubtful members.

We acknowledge the excellent recommendations of an unknown referee, which certainly improved the final version. The use of NASA's SkyView facility (<http://skyview.gsfc.nasa.gov>) located at NASA Goddard Space Flight Center, and the gallery image of NOAO ([http://www.noao.edu/image\\_gallery/html/im0423.html](http://www.noao.edu/image_gallery/html/im0423.html)), together with the technical support and hospitality at CASLEO during the observing runs, are also acknowledged. Special thanks go to Dr. Hugo G. Marraco for his useful comments.

## REFERENCES

- Aidelman, Y., Cidale, L. S., Zorec, J., & Arias, M. L. 2012, *A&A*, 64
- Arp, H. C. & van Sant, C. T. 1958, *AJ* 63, 341
- Axon, D. J., & Ellis, R. S. 1976, *MNRAS* 177, 499
- Beer A. 1961, *CoCam* 44, 143
- Bergeat, J., Sibille, F., Lunel, M., & Lefebvre, J. 1976, *A&A* 52, 227
- Bjorkman, K. S. 2011, in *Interactin Binaries to Exoplanets: Essential modeling Tools*, Proceedings IAU Symp. No. 282, page. 173. Mercedes T. Richards & Ivan Hubeny, eds.
- Bonatto, C., Bica, E., Ortolani, S., & Barbuy, B. 2006, *A&A* 453, 121
- Cannon, A. J., & Mayall, W. M. 1949, *Ann. Harvard coll. Obs* 112 Henry Draper extension 2
- Capps, R. W., Coyne, G. V., & Dyck, H. M. 1973, *ApJ* 184, 173
- Clarke, D. 1986, *A&A* 161, 412
- Coyne, G. V. 1976b, *A&A* 49, 89
- Coyne, G. V., & Kruszewski, A. 1969, *AJ* 74, 528
- Coyne, G. V., & Vrba, F. J. 1976, *ApJ* 207, 790
- Dachs, J., & Kaiser, D. 1984, *A&AS* 58, 411

- Evans, C. J., Smartt, S. J., Lee, J-K, et al. 2005, *A&A* 437, 467
- Feast, M. W. 1963, *MNRAS* 126, 11
- Garrison, R. F., Hiltner, W. A., & Schild, R. E. 1977, *ApJS* 35, 111
- Hernández, C. 1960, *Boletín de la Asociación Argentina de Astronomía* 2, 46
- Hiltner, W. A., Garrison, R. F., & Schild, R. E. 1969, *ApJ* 157, 313
- Houck, N., & Cowley A. P. 1975, Michigan Spectral survey, Ann Arbor, Dep. Astron., Univ. Michigan, I
- Hsu, J-C, & Breger 1982, *ApJ* 262, 732
- Jakate, S. M. 1978, *AJ* 83, 1179
- Lynga, G. in *Catalog of Open Clusters Data*, Computer Based Catalogue available through the CDS, Strasbourg, France, and NASA DATA Center, Greenbelt, Maryland, USA, , 5th. edition 4, 121
- Magalhães, A. M., Benedetti, E., & Roland, E. H. 1984, *PASP* 96, 383
- Manset, N., & Bastien, P. 2001, *AJ* 122, 3453
- Maronna, R., Feinstein, C., & Clocchiatti, A. 2002, *A&A* 260, 525
- Marraco, H. G., Vega, E. I., & Vrba, F. J. 1993, *AJ* 105, 258
- Martínez, E., Aballay, J. L., Marún, A., & Ruartes, H. 1990, *Bol. Asoc. Arg. de Astronomia* 36, 342
- McSwain M. V., & Gies, D. R. 2005b, *ApJS* 161, 118
- McSwain M. V., Huang, W. & Gies, D. R. 2009, *ApJ* 83, 1179
- Odell, A. P. 1979, *PASP* 91, 326
- Orsatti, A. M., Vega, E. I., & Marraco, H. G. 2000, *A&A* 144, 202
- Orsatti, A. M., Vega, E. I., & Marraco, H. G. 2006, *AJ* 132, 1783
- Orsatti, A. M., Feinstein, C., Vergne, M. M., Martinez, R. E., & Vega, E. I. 2010, *A&A* 513, A75
- Orsatti, A. M., Vega, E. I., & Marraco, H. G. 1998, *AJ* 116, 266
- Poeckert, R., Bastien, P., & Landstreet, J. D. 1979, *AJ* 84, 812
- Rufener, F., & Bartholdi, P. 1982, *A&AS* 48, 503
- Sagar, & Cannon, R. D. 1995, *A&AS* 111, 75
- Schild, R. E. 1970, *ApJ* 161, 855
- Schmidt-Kaler, Th. 1982, In: *Landolt/Bornstein, Neue Series VI / 2b*
- Serkowski, K. 1968, *ApJ* 154, 115
- Serkowski, K. 1970, *ApJ* 160, 1083
- Serkowski, K. 1973, in *IAU Symp. 52*, Greenberg, J. M. & van der Hulst, H. C., (eds) in “Interstellar Dust and Related Topics”, Reidel, Dordrecht-Holland, p. 145
- Serkowski, K., Mathewson, D. L. & Ford, V. L. 1975, *ApJ* 196, 261
- Stankov, A., Handler, G., Hemper, M. & Mettermayer, P. 2002, *MNRAS* 336, 189
- Turnshek, D. A., Bohlin, R. C., Williamson, R. L., Lupie, O. L., Koornneef, J., & Morgan, D. H. 1990, *AJ* 99, 1243
- Watson, R. D. 1983, *ApSS* 92, 293
- Whittet, D. C. B., Martin, P. G., Hough, J. H., Rouse, M. F., Bailey, J. A. & Axon, D. J. 1992, *Ap. J.* 386, 562

- R. E. Martínez: Facultad de Ciencias Astronómicas y Geofísicas, Universidad Nacional La Plata, C.P. 1900, La Plata, Argentina (ruben@fcaglp.unlp.edu.ar).
- A. M. Orsatti: Facultad de Ciencias Astronómicas y Geofísicas, Universidad Nacional La Plata, C.P. 1900, La Plata, Argentina (ana\_orsatti@hotmail.com).
- E. I. Vega: Facultad de Ciencias Astronómicas y Geofísicas, Universidad Nacional La Plata, C.P. 1900, La Plata, Argentina (irene@fcaglp.unlp.edu.ar).